



# Macrophage Transactivation for Chemokine Production Identified as a Negative Regulator of Granulomatous Inflammation Using Agent-Based Modeling

Daniel Moyo<sup>1,2</sup>, Lynette Beattie<sup>1†</sup>, Paul S. Andrews<sup>3,4</sup>, John W. J. Moore<sup>1</sup>, Jon Timmis<sup>3,4</sup>, Amy Sawtell<sup>1</sup>, Stefan Hoehme<sup>5</sup>, Adam T. Sampson<sup>6</sup> and Paul M. Kaye<sup>1\*</sup>

<sup>1</sup>Centre for Immunology and Infection, Department of Biology and Hull York Medical School, University of York, York, United Kingdom, <sup>2</sup>Department of Computer Science, University of York, York, United Kingdom, <sup>3</sup>Department of Electronics, University of York, York, United Kingdom, <sup>4</sup>SimOmics Ltd., York, United Kingdom, <sup>5</sup>Institute for Computer Science, University of Leipzig, Leipzig, Germany, <sup>6</sup>Division of Computing and Mathematics, Abertay University, Dundee, United Kingdom

## OPEN ACCESS

### Edited by:

Takayuki Yoshimoto,  
Tokyo Medical University, Japan

### Reviewed by:

Francesco Pappalardo,  
Università degli Studi di Catania, Italy  
Shinichi Hashimoto,  
Kanazawa University, Japan

### \*Correspondence:

Paul M. Kaye  
paul.kaye@york.ac.uk

### †Present address:

Lynette Beattie,  
Doherty Institute, University of  
Melbourne, Melbourne, VIC, Australia

### Specialty section:

This article was submitted to  
Inflammation,  
a section of the journal  
Frontiers in Immunology

**Received:** 07 January 2018

**Accepted:** 14 March 2018

**Published:** 27 March 2018

### Citation:

Moyo D, Beattie L, Andrews PS,  
Moore JWW, Timmis J, Sawtell A,  
Hoehme S, Sampson AT and  
Kaye PM (2018) Macrophage  
Transactivation for Chemokine  
Production Identified as a Negative  
Regulator of Granulomatous  
Inflammation Using Agent-Based  
Modeling.  
Front. Immunol. 9:637.  
doi: 10.3389/fimmu.2018.00637

Cellular activation *in trans* by interferons, cytokines, and chemokines is a commonly recognized mechanism to amplify immune effector function and limit pathogen spread. However, an optimal host response also requires that collateral damage associated with inflammation is limited. This may be particularly so in the case of granulomatous inflammation, where an excessive number and/or excessively florid granulomas can have significant pathological consequences. Here, we have combined transcriptomics, agent-based modeling, and *in vivo* experimental approaches to study constraints on hepatic granuloma formation in a murine model of experimental leishmaniasis. We demonstrate that chemokine production by non-infected Kupffer cells in the *Leishmania donovani*-infected liver promotes competition with infected KCs for available iNKT cells, ultimately inhibiting the extent of granulomatous inflammation. We propose trans-activation for chemokine production as a novel broadly applicable mechanism that may operate early in infection to limit excessive focal inflammation.

**Keywords:** kupffer cells, granulomas, inflammation, *Leishmania*, natural killer T cells, agent-based modeling, computational immunology, liver

## INTRODUCTION

Immune responses are commonly initiated by localized infectious insult and multiple mechanisms have evolved to allow spread of host effector responses to meet the challenge of pathogen containment. In the late 1950s, seminal studies by Isaacs and Lindenmann defined how “interferons” amplified local cellular resistance following virus infection (1, 2). A decade later, Mackaness described cross protective cellular immunity mediated *via* T cell cytokine-dependent macrophage activation (3). More recently, cytokine- and chemokine-mediated amplification of host protective immunity has been described across a spectrum of responses driven by both innate lymphoid cells and *via* conventional T cells (4–9). While serving to eliminate pathogens more effectively, a potentially undesirable consequence of amplifying immune effector responses is immunopathology, collateral damage induced by an overzealous drive toward inflammation. Hence, an equally impressive array of “regulatory” or “suppressive” mechanisms have been defined that serve to limit immunopathology, and that suggest an evolutionary balance between pathogen elimination and host survival (10–12).

Granulomatous inflammation represents an extreme form of focal inflammation, often initiated around pathogens or foreign bodies that pose a formidable challenge for immune clearance. Granulomas are a hallmark of the immunopathology of many human infectious diseases including tuberculosis (13, 14), schistosomiasis (15), and leishmaniasis (16). While granuloma formation may provide means for containment and be host beneficial, excessive granuloma formation, numerically or in terms of individual granuloma size can lead to severe pathological consequences. Hence, mechanisms for limiting the exuberance of the granulomatous response through late acting regulatory pathways are also well described in the literature (17–20). However, the question of whether additional regulatory mechanisms operate at the earliest stages of granuloma initiation and prevent or limit over-exuberant granuloma formation has not been previously addressed.

Experimental visceral leishmaniasis, resulting from infection of mice with the Kupffer cell (KC) tropic parasite *Leishmania donovani*, has provided a highly tractable tool to study the initiation of granulomatous pathology in the hepatic microenvironment. Following infection of mice with *L. donovani*, infected KCs transiently release the chemokines CCL1, CCL2, and CXCL10 in a T cell-independent manner, whereas sustained expression of CXCL10 is dependent upon IFN $\gamma$  production by invariant NKT (iNKT) cells (21). IFN $\gamma$  production by iNKT cells is in turn costimulated by ligation of CD47 on natural killer T (NKT) cells by signal regulatory protein alpha (SIRP $\alpha$ ) expressed on KCs, providing positive feedback for sustained iNKT cell recruitment and KC activation (22). A similar role for CXC chemokines in recruiting hepatic NKT cells has been observed in other models of liver infection/inflammation (23, 24). For example, CXCL9 produced by KCs following infection with the bacterium *Borrelia burgdorferi* results in CXCR3-dependent clustering of NKT cells around infected KCs (25), whereas CXCR6 and its ligand CXCL16 regulate NKT cell accumulation in the liver during fibrosis (26). Hence, early recruitment of “amplifier” cells such as NKT cells is a central and common theme of focal inflammation.

Examination of the kinetics of granulomatous inflammation in this model of visceral leishmaniasis suggests, however, that there may be inherent limitations imposed on the ability of the host to form hepatic granulomas. Notably, granuloma formation proceeds asynchronously, and even many weeks after infection, fully formed granulomas sit side by side with infected KCs that appear to have failed to stimulate an inflammatory focus (16, 27). Here, we have combined transcriptional profiling and computational modeling to probe possible mechanisms that might underpin the asynchronous development of granulomas in this model. We demonstrate that KC chemokine production, contrary to expectations, is not restricted to infected cells alone, but spreads in trans to include uninfected KCs within the infected liver. Data generated using a novel agent-based model (ABM) in which KCs and iNKT cells interact within a spatially constrained sinusoidal network suggest that the spreading of chemokine production to uninfected KCs limits the competitiveness of infected KCs in terms of their ability to attract iNKT cells and initiate granuloma formation. *In silico* experiments predicted that this competition could be overcome by increasing the number of available

NKT cells, a prediction borne out *in vivo*. Hence, our data identify a new pathway that operates early in infection to limit excessive inflammation by introducing competition for a finite resource (i.e., iNKT cells) that is needed for granuloma initiation.

## MATERIALS AND METHODS

### Mice and Parasites

C57BL/6 mice were obtained from Charles River (UK). mT/mG (28) and LysMcre (29) mice have been previously described. Mice were bred and housed under specific pathogen-free conditions and used at 6–12 weeks of age. The tandem Tomato fluorescent protein expressing Ethiopian strain of *L. donovani* (tdTom. LV9) (30) was maintained by serial passage in *Rag1*<sup>-/-</sup> mice. Amastigotes were isolated from infected spleens, and mice were infected with  $3 \times 10^7$  *L. donovani* amastigotes intravenously (i.v.) via the tail vein in 200  $\mu$ l of RPMI 1640 (GIBCO, UK). All animal procedures were approved by the University of York Animal Welfare and Ethical Review Board and carried out under UK Home Office license (PPL 60/4377).

### Microarray Analysis

As previously described (31), KCs were flow sorted (on the basis of SSC/FSC and expression of CR1g, Gr-1 and F4/80) from naive mice and from infected mice and KCs from infected mice were further sorted (on the basis of TdTomato expression) into those containing amastigotes (“infected”) and those that did not (“inflamed”). A total of 64 mice were used in the microarray study, in four independent infection experiments. RNA was isolated, amplified, and equal amounts were assayed using Agilent SurePrint G3 Gene Expression 8  $\times$  60 Microarray chips. Scanned data were normalized (80th percentile) and gene expression data analyzed using Genespring v9. Differentially expressed (DE) genes were defined using a false discovery rate (FDR) of 5%. Source data are accessible from EBI Array Express (E-MEXP-3877) and methodology for subsequent data analysis is described in further detail elsewhere (31).

### Histological Analysis

Mice were treated with 1  $\mu$ g recombinant IL-15 (BioLegend) intravenously and infected 3 days later. Four days postinfection, mice livers were extracted, weighed, and then placed into 2% PFA in PBS for 2 h, then 30% sucrose in PBS overnight. Tissues were then embedded in optimal cutting temperature (Sakura) and stored at  $-70^{\circ}\text{C}$  until use. 10  $\mu$ m cryosections were fixed and labeled with Alexa647 or Alexa488 conjugated F4/80 (eBioscience) and DAPI (Invitrogen) to visualize KCs and cell nuclei, respectively. Images were captured as 0.81  $\mu$ m optical slices using a LSM510 confocal microscope (Zeiss). Blinded slides were imaged to score the percentage of infected foci having formed a distinct inflammatory focus (greater than 15 cells), with imaging fields selected *via* tdTomato expression.

### Flow Cytometry

Livers were homogenized and mononuclear cells prepared as previously described (30). Cells were incubated with anti-CD16/32

and then labeled with NK1.1, CD3, B220, and CD1d tetramer (a kind gift from V. Cerundolo) to identify T, NK, and NKT cells. Samples were analyzed using a CyAn flow cytometer with Summit software (DAKO). Autofluorescent events and dead cells were excluded from analysis by gating on unused fluorescent channels and LIVE/DEAD fixable dead cell stain (Invitrogen), respectively.

## Parameterizing and Calibrating the Simulation

A full summary of the biological data available that was used to calibrate the simulation is listed in Table S1 in Supplementary Material. The entire list of baseline simulation parameters is found in Table S3 in Supplementary Material. Full details of parameterization and calibration of the simulation are provided in the Supplemental Experimental Procedures.

## Statistical Analysis

When quantifying granulomas, experimental data are expressed as mean  $\pm$  SEM for each group of five mice from two independent experiments, and statistical analyses performed using two-tailed paired Student's *t*-tests. All tests used 95% confidence intervals. Simulation data non-normality was determined using the D'Agostino and Pearson test, and non-normal simulation data were analyzed using either Wilcoxon signed-rank or Kolmogorov–Smirnov tests where appropriate. Aleatory analysis was used to determine the minimum number of simulation results required to mitigate stochastic uncertainty (see Figure S4 in Supplementary Material). Latin-hypercube sensitivity analysis was facilitated by using the Spartan tool for understanding uncertainty in simulations (32).

## RESULTS

### Chemokine Production by KCs in Mice Infected With *L. donovani*

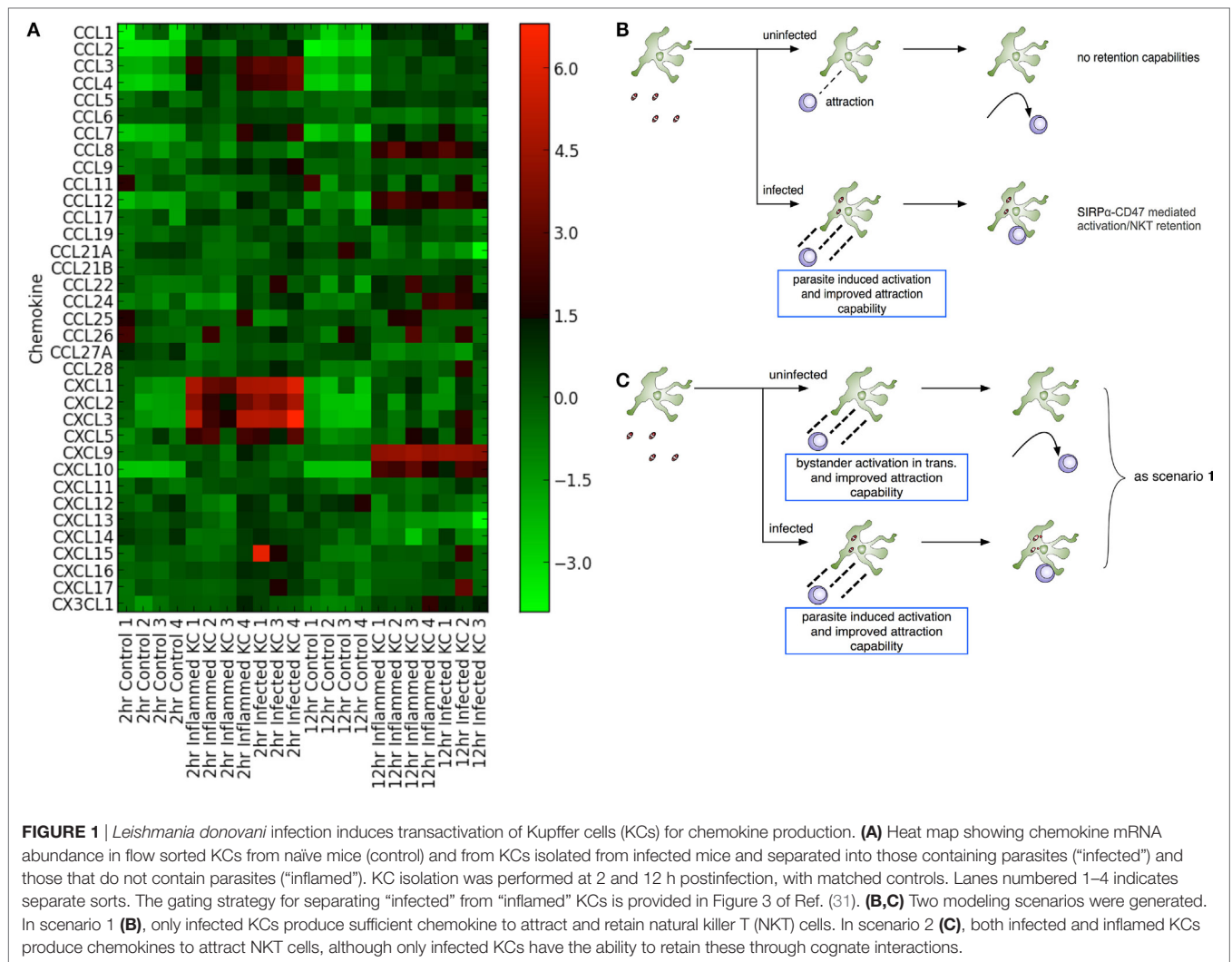
Both chemokines and iNKT cells are central to the initiation of granulomatous inflammation following *L. donovani* infection. In order to gain insight into the production of chemokines involved in KC-directed recruitment of NKT cells, we used transcriptional profiling of KCs isolated from mice infected with *L. donovani* as previously described (31). Following infection of mice with Td-tomato transgenic *L. donovani*, approx. 20% of the KC population are infected with amastigotes. We isolated KCs from infected mice and sort purified these KCs on the basis of whether they contained intracellular amastigotes (“infected”) or not (herein referred to as “inflamed”) to denote their exposure to inflammatory signals *in vivo* (31). As shown in **Figure 1A**, KCs from infected mice expressed a variety of chemokines when compared to KCs isolated from naïve mice. At 2 h post infection (p.i.), enhanced accumulation of mRNAs for *Cxcl1*, *Cxcl2*, *Cxcl3*, and *Cxcl5*, as well as *Ccl3* and *Ccl4*, was evident (determined as differentially expressed using a 5% FDR). This transcriptional response was transient, in keeping with previous studies at the level of whole liver tissue (21). Rapid secretion of chemokines in response to *L. donovani* infection can also be inferred from studies in which G-protein coupled receptor signaling was abrogated by pertussis

toxin (22). A suite of inducible chemokines, including *Cxcl9*, *Cxcl10*, *Ccl8*, and *Ccl12* showed enhanced mRNA accumulation at 12 h p.i. (at a 5% FDR), again in keeping with data in whole liver and with previously published data indicating the production of IFN $\gamma$  by iNKT cells during early *L. donovani* infection [e.g., Figure 2 in Ref. (22)]. For example, qRT-PCR demonstrated sustained and elevated *Cxcl10* at 24 h p.i. (33). Similarly, transcriptional profiling of the livers of infected BALB/c mice ( $n = 4\text{--}5$  per time point) indicates sustained elevation of *Cxcl9* (Log<sub>2</sub>FC compared to controls of 5.25, 5.14, 5.34, and 4.74 for days 15, 21, 36, and 42 p.i., respectively; FDR 0.05,  $p < 0.05$ ) and *Cxcl10* (Log<sub>2</sub>FC of 4.84, 4.92, 5.36, and 4.55, respectively; Ashwin et al., manuscript in preparation). Strikingly, there was little difference to discriminate the chemokine response of infected vs. inflamed KCs, although we cannot rule out different degrees of posttranscriptional regulation of chemokine secretion in infected vs. inflamed KCs (34). Collectively, our data suggest that although initiated by infection, production of chemokines rapidly spreads in trans throughout the liver KC network.

Chemokine induction by infected cells is thought to provide a means for focal inflammation, the recruitment of additional leukocytes in an ordered manner being essential for granuloma formation and the ultimate activation of macrophage host defense mechanisms. However, given this argument, these data appear counterintuitive. In order to try to understand how transactivation for chemokine production might influence the generation of focal inflammation, and given the absence of tools to selectively and directly manipulate chemokine production by infected vs. uninfected KCs *in vivo*, we adopted an *in silico* experimental approach conducive to testing a variety of different hypotheses (**Figures 1B,C**).

### An ABM of the Hepatic Sinusoidal Microenvironment

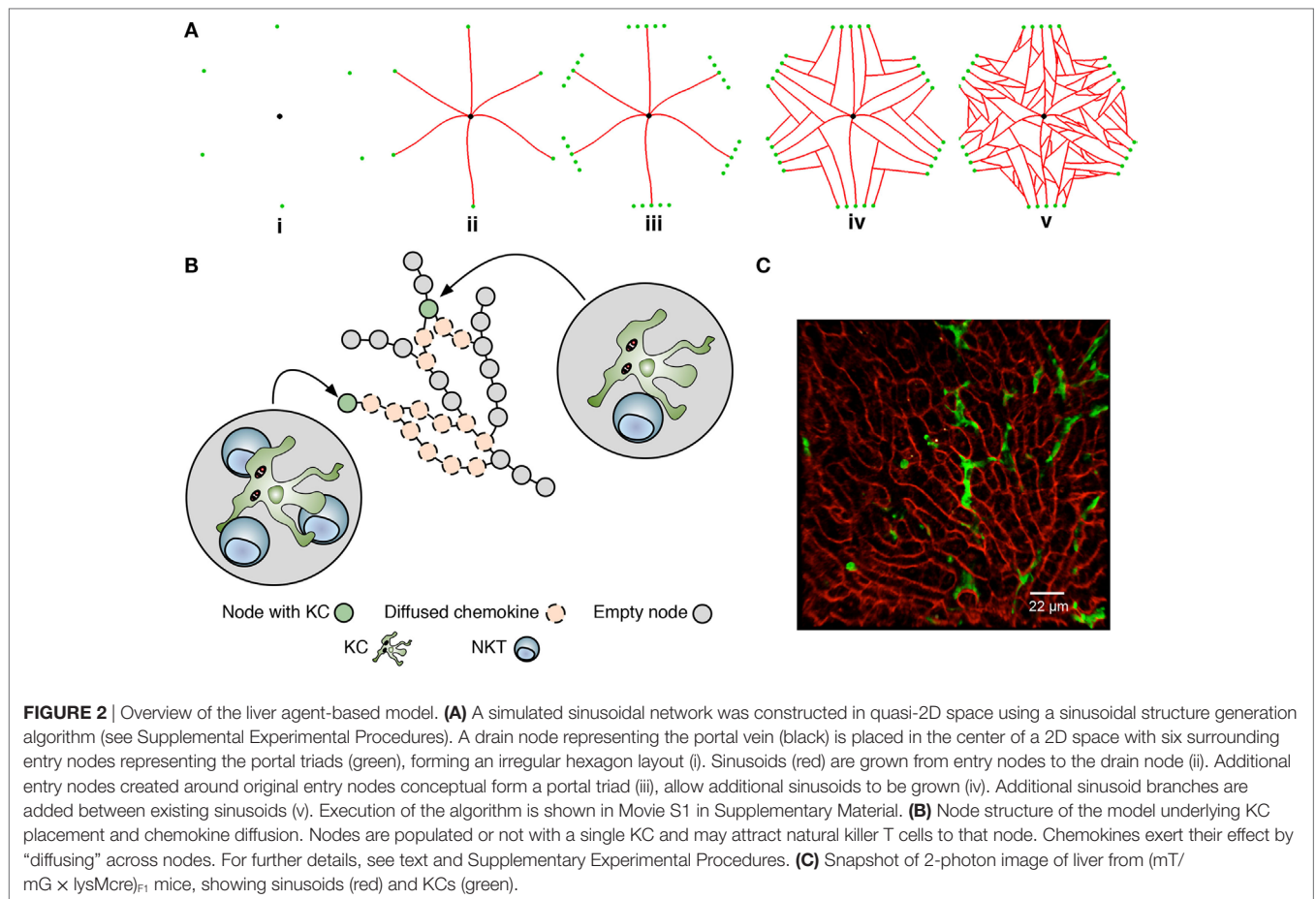
Agent-based models, where rule-driven “agents” can represent a cell or lower-scale entities of interest, are naturally suited to simulating inflammation in a spatially constrained environment (35–37). To construct this environment, we used published 3D data describing the overall size of lobules, the average non-branched sinusoid length, and the branching angles between sinusoids (38) as the basis for developing a novel algorithm to generate statistically realistic liver lobule sections similar to that reported recently (39). A range of quasi-2D sinusoidal network structures, where each structure can be considered as a slice through a 3D lobule, was created using a multi-stage generative algorithm augmented with these data (38) (**Figure 2A**; Movie S1, Figures S1A–D, Table S1, and Supplementary Experimental Procedures in Supplementary Material). The resulting networks (**Figure 2B**), represented as graphs of nodes connected by edges, serve as discrete spatial simulation environments that mimic the sinusoidal structure observed in live mice imaged by 2-photon intra-vital microscopy in (mT/mG  $\times$  lysMcre)<sub>F1</sub>, as previously described (30) (**Figure 2A** vs **Figure 2C**). Analysis (by Pearson correlation coefficients and Kolmogorov–Smirnov tests) using 10 independently generated structures indicated that variance in structure *per se* had minimal impact on the results of subsequent simulations (see below).



We defined where and how cellular interactions were allowed to occur within our simulation environment based on three different types of network node: periportal nodes, located at the peripheries of the structure allow NKT cells to enter and exit the simulated lobule section; regular-nodes, capable of holding a single KC and any number of NKT cells; and a single centrilobular-node, representing the central vein where NKT cells could exit the structure. Only NKT cells were capable of movement within the structure. KCs remain immobile, as reported in early stages of infection with *B. bugdorferi* (25), BCG (40), and *L. donovani* (30). Our KC placement algorithm distributes KCs in periportal, midzonal, and centrilobular locations in a ratio of 4:3:3, based on Ref. (41, 42). As centrilobular KCs have reduced phagocytic capability compared to periportal KCs (41), the distribution of infected KCs in our simulation is 65% periportal, 25% midzonal, and 10% centrilobular for the purposes of experimentation.

A detailed description of the model and key assumptions is provided in the Supplemental Experimental Procedures and Tables S2 and S3 in Supplementary Material. State diagrams written in the Unified Modeling Language that illustrate the behavior associated with KCs and NKT cells are provided in

Figure S2 in Supplementary Material. Briefly, mechanisms of cellular attraction and retention were modeled generically, since the precise function, functional overlap, and interaction between distinct chemokines has yet to be fully elucidated. For the purposes of the current abstraction, we refer to the chemokines as attractive and retentive, being independent and quantitatively distinct and with discrete areas of influence. The simulation was constructed to allow both a minimum and a maximum diffusion distance to be parameterized for all chemo-attractants produced by KCs. NKT cells traverse the sinusoidal network at 10–20  $\mu\text{m}/\text{min}$  with a random walk behavior (25), with no enforcement of directionality unless under the attractive influence of KC-derived chemokines. Strength of attraction is modeled as a function of distance from the source KC. Upon interaction with infected KCs, NKT cells produce  $\text{IFN}\gamma$  (as a representation of all macrophage-activating cytokines) following cognate receptor engagement (22), facilitating KC activation and NKT cell arrest (25, 43). Our previous data on  $\text{SIRP}\alpha$ -CD47 have suggested that cognate receptor–ligand interactions also regulate NKT cell retention on infected KCs, with the induced expression of  $\text{SIRP}\alpha$  after infection being preferentially, but not exclusively observed



on infected KCs (22). In our model, this interaction is used to represent a cognate retention signal, but this reflects an abstraction of what may be potentially much more complex interactions. The amplification of KC-derived attractive chemokines through this process can lead to the accumulation of multiple NKT cells at a given KC (referred to here as “inflammatory foci”). It is assumed that through the sum of all KC–NKT cell interactions within an inflammatory focus, a threshold for granuloma formation and the subsequent recruitment of additional leukocytes associated with maturing granulomas (including B cells, T cells, monocytes, and NK cells) is reached, but these cells and processes are not explicitly modeled. We have also not modeled the ultimate microbicidal activity of these granulomas.

### Parasite-Induced Activation of Infected KCs With/Without Bystander Chemokine Production by Uninfected KCs

Two experimental scenarios were devised to investigate the influence of varying both infected and inflamed KC function. Scenario 1 (**Figure 1B**) was constructed to restrict chemokine production to infected KCs only, and scenario 2 (**Figure 1C**) to investigate the impact of transactivation of KC for chemokine production. As KC activation of NKT cells is optimal in the presence of cognate interactions (22), our model assumes these are a requirement for

retention; hence, only infected KCs can generate stable inflammatory foci, and these foci, for the purposes of the model, are composed only of NKT cells and KCs. In contrast, inflamed KCs in scenario 2 might act as potential competitors for available NKT cells, being able to attract but not retain them. Although this model can be used to probe a variety of different potential questions related to the initiation of granuloma formation (see Discussion), we focus here on a factorial analysis that involved simultaneously modifying the simulation parameters related to chemokine diffusion distance, time required to activate KCs, and time for KCs to reach maximal chemokine production.

First, we quantified the influence of distance from effect on attraction. Factorial analysis, modifying the maximum diffusion distance of chemokine, showed that greater chemokine diffusion distance leads to increased percentages of infected KCs forming inflammatory foci in both scenarios (**Figures 1B,C**), whether those foci were qualified as containing 4, 6, or 8 NKT cells. However, our simulation predicted diminishing returns when increasing maximum diffusion past ~120  $\mu\text{m}$  (Figure S1E in Supplementary Material). Thus, significant differences ( $P \leq 0.001$ ) were observed when comparing the frequency of inflammatory foci that resulted from each increase in diffusion distance against the previous distance (e.g., 20–30  $\mu\text{m}$ :  $P = 0.001216$ , 30–40  $\mu\text{m}$ :  $P = 0.000019$ ). However, when increasing from 120 to 130  $\mu\text{m}$  and beyond, the increase in inflammatory foci was not significant ( $P = 0.312$ ).

Interestingly, this tipping point is close to the  $\sim 100 \mu\text{m}$  reported as the distance of a functional chemokine gradient *in vivo* (44). These results suggest that if it were possible to selectively increase chemokine diffusion *via* increased production (or other means) by infected KCs compared to inflamed KCs, or conversely decrease chemokine diffusion by inflamed KCs, infected KCs would gain competitive advantage in terms of attracting NKT cells.

We next compared our two experimental scenarios in terms of total stimulation time (i.e., a measure of activation) received by the entire infected KC population, and the frequency of inflammatory foci formed associated with that population. **Figure 3A** illustrates a response curve for scenario 1 showing the total stimulation time received by all infected KCs, across a range of the two main parameters that determine KC activation dynamics—the time required to activate KCs and the duration KCs remain activated. When comparing this response landscape of scenario 1

with that generated in scenario 2 (**Figure 3C**), there was a marked reduction in stimulation time received overall by infected KCs in scenario 2 compared to scenario 1. This trend is also observable when comparing the percentage of inflammatory foci, whether qualified at 8 NKT cells (**Figure 3B** for scenario 1 and **Figure 3D** for scenario 2) or at 4 or 6 NKT cells (data not shown).

Together, these results demonstrate that in comparison to chemokine production restricted to infected KCs, additional chemokine production by inflamed KC generates a less focused inflammatory response, measured either by frequency of infected KC that form inflammatory foci, or by stimulation time received by infected KCs. This result most likely reflects the liver lobule becoming saturated with attractive chemokines derived from both inflamed and infected KCs in scenario 2, reducing the competitiveness of infected KCs to selectively recruit NKT cells. In other words, chemokine production by inflamed KC acts in a

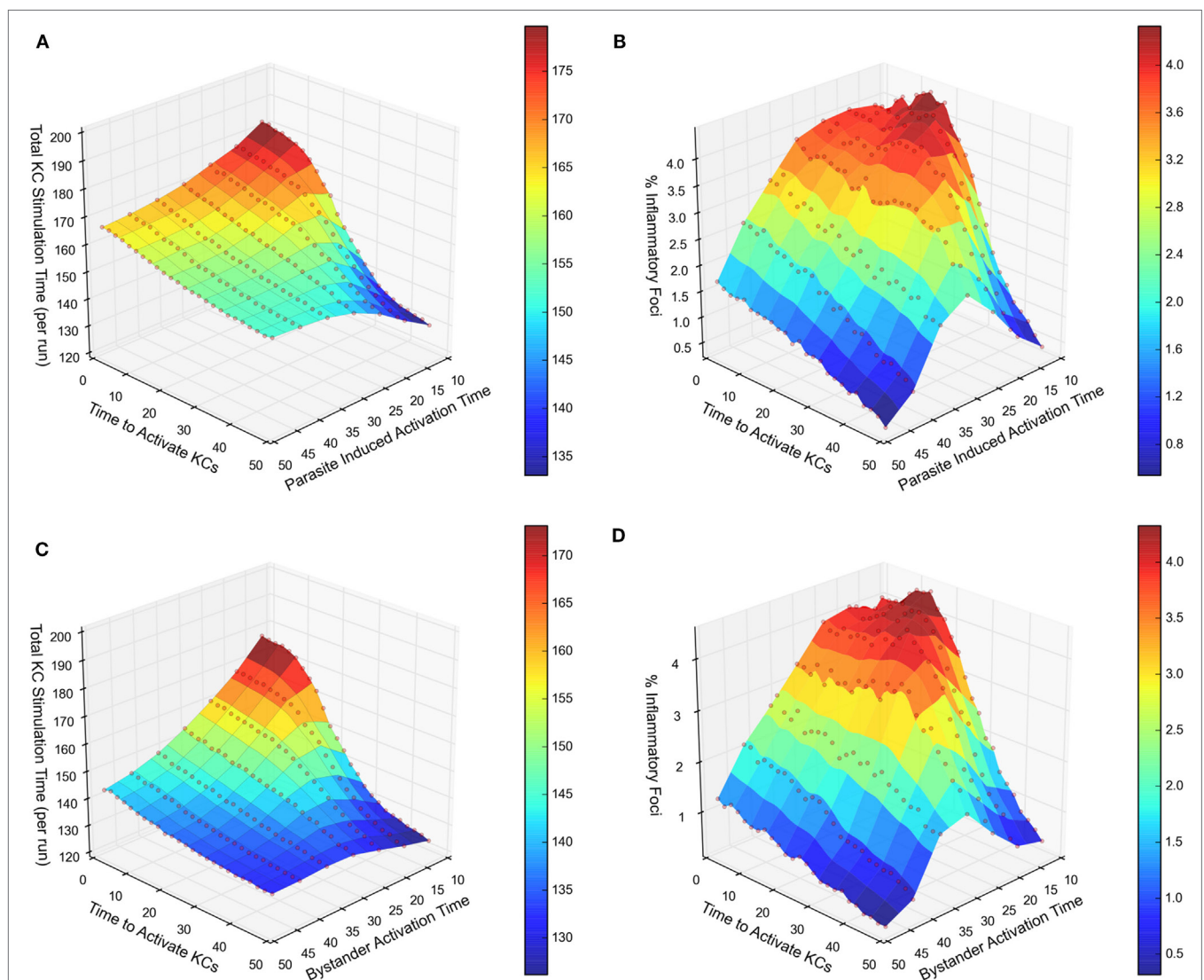


**FIGURE 3** | Response landscapes for parasite-induced KC activation with and without KC activation in trans. **(A–D)** Two-at-a-time (TAT) parameter analysis showing the effect on total KC stimulation time **(A,C)** and on % inflammatory foci **(B,D)** of modifying either cumulative time to activate KCs and parasite-induced activation time **(A,B)** or cumulative time to activate KCs and bystander activation time **(C,D)**. For further details, see Supplementary Experimental Procedures.

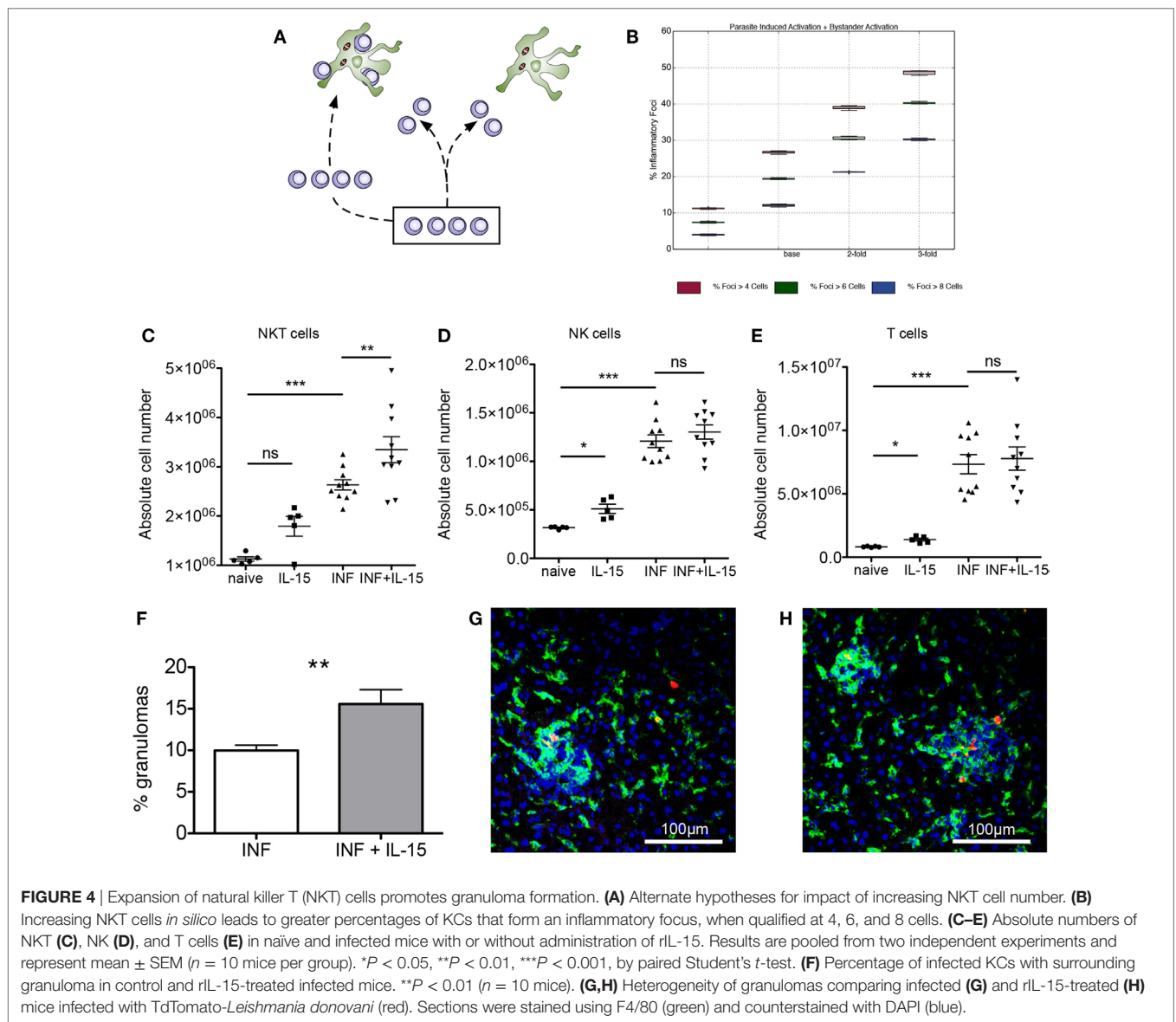
negative immune regulatory manner, limiting the extent of the inflammatory response around infected KCs.

## Increasing NKT Cell Numbers Overcomes Bystander Regulation

We then investigated how modifying the target of this competition affected the quantity and quality of inflammatory foci generated. We hypothesized that altering NKT cell frequency might result in either (i) similarly abundant foci, but with each being more substantive in terms of NKT cellularity or (ii) increased numbers of inflammatory foci, thus overcoming the competitive effect of bystander chemokine production by inflamed KCs (**Figure 4A**). Our simulation results showed that increasing NKT cell numbers above the calibrated value lead to significant increases in the frequency of inflammatory foci in scenario 1, a result that would be expected. Strikingly, an increase in frequency of inflammatory foci was also observed to be the case for scenario 2, regardless of

how we qualified focus size (**Figure 4B**). For example, with an increase in NKT cell availability of twofold, the number of inflammatory foci increased 1.5-fold, whereas increasing NKT cells by threefold doubled the frequency of inflammatory foci.

To test whether this predictive *in silico* data was also borne out *in vivo*, we treated mice for 3 days with recombinant IL-15 to induce increased NKT cell proliferation and survival (45) and then infected these mice with *L. donovani* and scored early granuloma formation. In uninfected mice, IL-15 treatment resulted in increased numbers of NKT cells (including CD1d restricted NKT cells), NK cells, and T cells (**Figures 4C–E**; Figures S3A–D in Supplementary Material). In infected mice, all cell types were already increased in number compared to naïve mice, and the effect of IL-15 pretreatment was limited to an increase in the number of NKT cells (**Figure 4C**). Similarly, IL-15 pretreatment had no effect on the relative frequency of NK cells and T cells (Figures S3B,C in Supplementary Material) but resulted in an



increase in the relative frequency of NKT cells (from  $15.0 \pm 0.1$  to  $17.36 \pm 0.8\%$ ;  $n = 10$ ;  $P = 0.0043$ ; Figure S3E in Supplementary Material).

To ensure that we were scoring a biologically relevant histopathological response, while minimizing potential longer term effects of rIL-15 treatment, we chose to score the granulomas early in their development (day 4 p.i.) and define these as accumulations of 15 or more cells formed around an infected KC (not discriminating between NKT cells or other mononuclear cells). Although there was significant heterogeneity in size of these granulomas (Figures 4G,H), we found that the frequency of infected KCs that formed distinct granulomas was increased ~1.5-fold in mice pretreated with IL-15 and which had a higher number of NKT cells in the liver at the time of infection ( $P = 0.0038$ ; Figure 4F). Thus, treatment of mice with rIL-15, even under conditions where the increase in NKT cell number is relatively modest, leads to a significant enhancement in the frequency of infected KCs that can provide a nidus for granuloma formation.

## DISCUSSION

Granulomas represent a specialized form of inflammation that allows for the focal delivery of host effector responses and/or containment of pathogen products. While generally considered host beneficial, excessive granuloma formation may have significant pathological consequences. Here, we provide evidence that chemokine-dependent competition between infected and uninfected KCs for iNKT cells in the hepatic microenvironment acts as a natural attenuator of granuloma formation.

In models of experimental visceral leishmaniasis, granuloma formation is asynchronous, limiting the extent of hepatic inflammation, but also delaying parasite clearance (16, 27). A variety of different models could explain why isolated infected KCs can be found at times when other infected KCs are engaged in a fully mature granulomatous response. In a model of *Mycobacterium marinum*-induced granulomas in zebrafish, macrophage migration out of the granuloma has been observed (14, 46), and it is possible that infected KCs leave granulomas in mice infected with *L. donovani*. However, in both *L. donovani*-induced granulomas (30) and BCG-induced granulomas (40, 47) in immunocompetent mice, KCs appear to retain their characteristic lack of motility. Alternatively, there may be heterogeneity in KCs, a subset being more efficient in promoting granulomatous inflammation. Although we had previously modeled this possibility using an early version of our ABM (48), our recent studies evaluating differences between yolk-sac derived and bone marrow-derived KC indicate that both are competent to form granulomas and participate effectively in this response (49). A further possibility is that granuloma formation is rate limited by the availability of key amplifier cells. Experimental data to date indicate that iNKT cells play this role in experimental visceral leishmaniasis (22, 33, 50, 51), though we do not discount a role for other more recently identified innate lymphoid cells (52, 53).

Through transcriptional profiling, we demonstrated that both inflamed and infected KCs produce a variety of inducible chemokines able to attract NKT cells, suggesting the possibility that uninfected as well as infected KCs could compete for this

resource. However, as neither the mechanisms that regulate this transactivation nor experimental means to selectively regulate chemokine production by KCs are currently available, we adopted a computational approach to further explore this hypothesis. ABMs are well-suited toward studying tissue and cellular level inflammation (35–37). In constructing our ABM, we developed a novel algorithm for creating virtual sinusoidal networks that are visually representative of liver lobule sections, being defined by published statistics that captured the length between central vein and portal triad, average lengths of non-branched sinusoids and sinusoid branch angles (38). This represents an improvement on similar work (39). Our algorithm was not intended to produce a fully realistic whole lobule structure, but rather we were interested only in developing suitable quasi-2D vascular networks within liver lobules to provide an environment for the cellular and chemokine “agents” contained in the model. Similarly, while our ABM contained only three cellular agents (infected and inflamed KCs and NKT), this abstraction was nevertheless sufficient to probe previously inaccessible aspects of the underlying biology.

Our *in silico* results predicted that chemokine diffusion plays an important role in regulating the formation of inflammatory foci around infected KCs, though there are diminishing returns as a result of increased competition when lobules become flooded with chemokines. Subsequently, our model predicted an intuitive, but nonetheless previously unreported mechanism by which the production of NKT cell-attractive chemokines by inflamed KCs dampens the overall inflammatory response in the liver microenvironment, reducing the activation received by infected KCs. Our *in silico* data also predicted that this competition could be overcome by increasing the availability of NKT cells, and we were able to confirm that granuloma frequency can indeed be increased *in vivo* by increasing NKT cell numbers using rIL-15. The relationship between availability of NKT cells and an increase in the frequency of infected KCs generating granulomas has not previously been demonstrated.

Natural killer T cells represent a potent therapeutic target in a variety of clinical settings, due to their immune adjuvant function and production of various effector cytokines (54–57). Protective immunity associated with NKT cell activation has been reported in several disease settings. For example, V $\alpha$ 14 NKT cells activated by  $\alpha$ -galactosylceramide ( $\alpha$ -GalCer) have been shown to inhibit the development of malaria parasites in mice (58). Similarly, in a murine model of *Mycobacterium tuberculosis* infection,  $\alpha$ -GalCer-induced activation of NKT cells was associated with reduced bacterial loads, tissue injury, and improved mouse survival (59). Conversely, NKT cells have been implicated as key drivers of liver inflammation such as chronic liver injury (26). Although our results suggest that, in leishmaniasis, the initiation of granulomatous inflammation can be enhanced by increasing the availability of NKT cells, further long-term studies would be required to determine whether the host protective advantages of this intervention outweigh any possible pathological consequences.

It is important to recognize that our model has been developed to address early events in granuloma formation and does not take into account the potential for diversity in granuloma form and

function, including variations in microbicidal activity. These may be regulated *via* other aspects of the immune response that develop over time, and more complex models have been developed to address some of these issues (60). Redundancy of immune regulatory pathways is a common finding, and it is possible that other mechanisms come into play at later stages of granuloma evolution that affects the ability of KCs to recruit inflammatory cells and initiate granuloma formation. The kinetics of chemokine production is also likely to be highly dynamic, though in respect of CXCL9 and CXCL10, long-term transcriptomic profiling indicates that expression of these IFN $\gamma$ -inducible chemokines is sustained for at least 45 days postinfection (Ashwin et. al., unpublished).

In summary, our data argue that chemokine production by uninfected transactivated KCs provides an example of a novel negative regulatory mechanism to limit the impact of overzealous inflammatory responses that might otherwise lead to excess tissue pathology. Further studies to evaluate this hypothesis in a broader context of inflammation are clearly warranted.

## ETHICS STATEMENT

This study was carried out in compliance with the Animals (Scientific Procedures) Act 1986, under UK Home Office license PPL 60/4377. The protocol was approved by the University of York Animal Welfare and Ethical Review Board.

## REFERENCES

- Isaacs A, Lindenmann J. Virus interference. I. The interferon. *Proc R Soc Lond B Biol Sci* (1957) 147(927):258–67. doi:10.1098/rspb.1957.0048
- Isaacs A, Lindenmann J, Valentine RC. Virus interference. II. Some properties of interferon. *Proc R Soc Lond B Biol Sci* (1957) 147(927):268–73. doi:10.1098/rspb.1957.0049
- Mackaness GB. The influence of immunologically committed lymphoid cells on macrophage activity in vivo. *J Exp Med* (1969) 129(5):973–92. doi:10.1084/jem.129.5.973
- Chu T, Tyznik AJ, Roepke S, Berkley AM, Woodward-Davis A, Pattacini L, et al. Bystander-activated memory CD8 T cells control early pathogen load in an innate-like, NKG2D-dependent manner. *Cell Rep* (2013) 3(3):701–8. doi:10.1016/j.celrep.2013.02.020
- Griffith JW, Sokol CL, Luster AD. Chemokines and chemokine receptors: positioning cells for host defense and immunity. *Annu Rev Immunol* (2014) 32:659–702. doi:10.1146/annurev-immunol-032713-120145
- Lertmengkolchai G, Cai G, Hunter CA, Bancroft GJ. Bystander activation of CD8+ T cells contributes to the rapid production of IFN-gamma in response to bacterial pathogens. *J Immunol* (2001) 166(2):1097–105. doi:10.4049/jimmunol.166.2.1097
- Mantovani A, Sica A, Sozzani S, Allavena P, Vecchi A, Locati M. The chemokine system in diverse forms of macrophage activation and polarization. *Trends Immunol* (2004) 25(12):677–86. doi:10.1016/j.it.2004.09.015
- Polley R, Sanos SL, Prickett S, Haque A, Kaye PM. Chronic *Leishmania donovani* infection promotes bystander CD8+ T-cell expansion and heterologous immunity. *Infect Immun* (2005) 73(12):7996–8001. doi:10.1128/IAI.73.12.7996-8001.2005
- Tough DF, Borrow P, Sprent J. Induction of bystander T cell proliferation by viruses and type I interferon in vivo. *Science* (1996) 272(5270):1947–50. doi:10.1126/science.272.5270.1947
- Graham AL, Allen JE, Read AF. Evolutionary causes and consequences of immunopathology. *Ann Rev Ecol Evol Syst* (2005) 36:373–97. doi:10.1146/annurev.ecolsys.36.102003.152622
- Mills KH. Regulatory T cells: friend or foe in immunity to infection? *Nat Rev Immunol* (2004) 4(11):841–55. doi:10.1038/nri1485
- Sorci G, Cornet S, Faivre B. Immune evasion, immunopathology and the regulation of the immune system. *Pathogens* (2013) 2(1):71–91. doi:10.3390/pathogens2010071

## AUTHOR CONTRIBUTIONS

DM, PA, JT, LB, and PK designed the simulation model. DM implemented the simulation model. LB and PK designed the experimental study. DM, JM, LB, and AS performed experimental studies. SH provided data and input on model development. PA and AS designed and implemented the algorithm for the generation of the artificial sinusoid structures. DM, LB, PA, JT, and PK analyzed the data and wrote the manuscript.

## ACKNOWLEDGMENTS

This work was supported by grants from The Wellcome Trust and the British Medical Research Council (to PK; WT106203 and G1000230, respectively), and the Engineering and Physical Science Research Council (to JT and PA EP/E053505/1 and EP/E049419/1). JT is partly funded by the Royal Society. The authors thank Vincenzo Cerundolo for providing the CD1d tetramers.

## SUPPLEMENTARY MATERIAL

The Supplementary Material for this article can be found online at <https://www.frontiersin.org/articles/10.3389/fimmu.2018.00637/full#supplementary-material>.

- Dorhoi A, Kaufmann SH. Perspectives on host adaptation in response to *Mycobacterium tuberculosis*: modulation of inflammation. *Semin Immunol* (2014) 26(6):533–42. doi:10.1016/j.smim.2014.10.002
- Pagan AJ, Ramakrishnan L. Immunity and immunopathology in the tuberculous granuloma. *Cold Spring Harb Perspect Med* (2015) 5(9). doi:10.1101/cshperspect.a018499
- Hams E, Aviello G, Fallon PG. The schistosoma granuloma: friend or foe? *Front Immunol* (2013) 4:89. doi:10.3389/fimmu.2013.00089
- Kaye PM, Beattie L. Lessons from other diseases: granulomatous inflammation in leishmaniasis. *Semin Immunopathol* (2016) 38(2):249–60. doi:10.1007/s00281-015-0548-7
- Lundy SK, Lukacs NW. Chronic schistosome infection leads to modulation of granuloma formation and systemic immune suppression. *Front Immunol* (2013) 4:39. doi:10.3389/fimmu.2013.00039
- Maroof A, Beattie L, Zubairi S, Svensson M, Stager S, Kaye PM. Posttranscriptional regulation of I110 gene expression allows natural killer cells to express immunoregulatory function. *Immunity* (2008) 29(2):295–305. doi:10.1016/j.immuni.2008.06.012
- Mentink-Kane MM, Cheever AW, Thompson RW, Hari DM, Kabatereine NB, Vennervald BJ, et al. IL-13 receptor alpha 2 down-modulates granulomatous inflammation and prolongs host survival in schistosomiasis. *Proc Natl Acad Sci U S A* (2004) 101(2):586–90. doi:10.1073/pnas.0305064101
- Owens BM, Beattie L, Moore JW, Brown N, Mann JL, Dalton JE, et al. IL-10-producing Th1 cells and disease progression are regulated by distinct CD11c(+) cell populations during visceral leishmaniasis. *PLoS Pathog* (2012) 8(7):e1002827. doi:10.1371/journal.ppat.1002827
- Cotterell SE, Engwerda CR, Kaye PM. *Leishmania donovani* infection initiates T cell-independent chemokine responses, which are subsequently amplified in a T cell-dependent manner. *Eur J Immunol* (1999) 29(1):203–14. doi:10.1002/(SICI)1521-4141(199901)29:01<203::AID-IMMU203>3.0.CO;2-B
- Beattie L, Svensson M, Bune A, Brown N, Maroof A, Zubairi S, et al. *Leishmania donovani*-induced expression of signal regulatory protein alpha on Kupffer cells enhances hepatic invariant NKT-cell activation. *Eur J Immunol* (2010) 40(1):117–23. doi:10.1002/eji.200939863
- Gupta G, Bhattacharjee S, Bhattacharyya S, Bhattacharya P, Adhikari A, Mukherjee A, et al. CXC chemokine-mediated protection against visceral leishmaniasis: involvement of the proinflammatory response. *J Infect Dis* (2009) 200(8):1300–10. doi:10.1086/605895

24. Sato T, Thorlacius H, Johnston B, Staton TL, Xiang W, Littman DR, et al. Role for CXCR6 in recruitment of activated CD8+ lymphocytes to inflamed liver. *J Immunol* (2005) 174(1):277–83. doi:10.4049/jimmunol.174.1.277
25. Lee WY, Moriarty TJ, Wong CH, Zhou H, Strieter RM, van Rooijen N, et al. An intravascular immune response to *Borrelia burgdorferi* involves Kupffer cells and iNKT cells. *Nat Immunol* (2010) 11(4):295–302. doi:10.1038/ni.1855
26. Wehr A, Baeck C, Heymann F, Niemietz PM, Hammerich L, Martin C, et al. Chemokine receptor CXCR6-dependent hepatic NK T Cell accumulation promotes inflammation and liver fibrosis. *J Immunol* (2013) 190(10):5226–36. doi:10.4049/jimmunol.1202909
27. Murray HW. Tissue granuloma structure-function in experimental visceral leishmaniasis. *Int J Exp Pathol* (2001) 82(5):249–67. doi:10.1046/j.1365-2613.2001.00199.x
28. Muzumdar MD, Tasic B, Miyamichi K, Li L, Luo L. A global double-fluorescent Cre reporter mouse. *Genesis* (2007) 45(9):593–605. doi:10.1002/dvg.20335
29. Clausen BE, Burkhardt C, Reith W, Renkawitz R, Forster I. Conditional gene targeting in macrophages and granulocytes using LysMcre mice. *Transgenic Res* (1999) 8(4):265–77. doi:10.1023/A:1008942828960
30. Beattie L, Peltan A, Maroof A, Kirby A, Brown N, Coles M, et al. Dynamic imaging of experimental *Leishmania donovani*-induced hepatic granulomas detects Kupffer cell-restricted antigen presentation to antigen-specific CD8 T cells. *PLoS Pathog* (2010) 6(3):e1000805. doi:10.1371/journal.ppat.1000805
31. Beattie L, d'El-Rei Hermida M, Moore JW, Maroof A, Brown N, Lagos D, et al. A transcriptomic network identified in uninfected macrophages responding to inflammation controls intracellular pathogen survival. *Cell Host Microbe* (2013) 14(3):357–68. doi:10.1016/j.chom.2013.08.004
32. Alden K, Read M, Timmis J, Andrews PS, Veiga-Fernandes H, Coles M. Spartan: a comprehensive tool for understanding uncertainty in simulations of biological systems. *PLoS Comput Biol* (2013) 9(2):e1002916. doi:10.1371/journal.pcbi.1002916
33. Svensson M, Zubairi S, Maroof A, Kazi F, Taniguchi M, Kaye PM. Invariant NKT cells are essential for the regulation of hepatic CXCL10 gene expression during *Leishmania donovani* infection. *Infect Immun* (2005) 73(11):7541–7. doi:10.1128/IAI.73.11.7541-7547.2005
34. Fan J, Heller NM, Gorospe M, Atasoy U, Stellato C. The role of post-transcriptional regulation in chemokine gene expression in inflammation and allergy. *Eur Respir J* (2005) 26(5):933–47. doi:10.1183/09031936.05.00120204
35. An G. Concepts for developing a collaborative in silico model of the acute inflammatory response using agent-based modeling. *J Crit Care* (2006) 21(1):105–10; discussion 110–1. doi:10.1016/j.jcrrc.2005.11.012
36. An G, Christley S. Addressing the translational dilemma: dynamic knowledge representation of inflammation using agent-based modeling. *Crit Rev Biomed Eng* (2012) 40(4):323–40. doi:10.1615/CritRevBiomedEng.v40.i4.70
37. Moore JW, Moyo D, Beattie L, Andrews PS, Timmis J, Kaye PM. Functional complexity of the *Leishmania granuloma* and the potential of in silico modeling. *Front Immunol* (2013) 4:35. doi:10.3389/fimmu.2013.00035
38. Hoehme S, Brulport M, Bauer A, Bedawy E, Schormann W, Hermes M, et al. Prediction and validation of cell alignment along microvessels as order principle to restore tissue architecture in liver regeneration. *Proc Natl Acad Sci U S A* (2010) 107(23):10371–6. doi:10.1073/pnas.0909374107
39. Wambaugh J, Shah I. Simulating microdosimetry in a virtual hepatic lobule. *PLoS Comput Biol* (2010) 6(4):e1000756. doi:10.1371/journal.pcbi.1000756
40. Egen JG, Rothfuchs AG, Feng CG, Winter N, Sher A, Germain RN. Macrophage and T cell dynamics during the development and disintegration of mycobacterial granulomas. *Immunity* (2008) 28(2):271–84. doi:10.1016/j.immuni.2007.12.010
41. Bouwens L, Baekeland M, De Zanger R, Wisse E. Quantitation, tissue distribution and proliferation kinetics of Kupffer cells in normal rat liver. *Hepatology* (1986) 6(4):718–22. doi:10.1002/hep.1840060430
42. Sleyster EC, Knook DL. Relation between localization and function of rat liver Kupffer cells. *Lab Invest* (1982) 47(5):484–90.
43. Geissmann F, Cameron TO, Sidobre S, Manlongat N, Kronenberg M, Briskin MJ, et al. Intravascular immune surveillance by CXCR6+ NKT cells patrolling liver sinusoids. *PLoS Biol* (2005) 3(4):e113. doi:10.1371/journal.pbio.0030113
44. Weber M, Hauschild R, Schwarz J, Moussion C, de Vries I, Legler DE, et al. Interstitial dendritic cell guidance by haptotactic chemokine gradients. *Science* (2013) 339(6117):328–32. doi:10.1126/science.1228456
45. Matsuda JL, Gapin L, Sidobre S, Kieper WC, Tan JT, Ceredig R, et al. Homeostasis of V alpha 14i NKT cells. *Nat Immunol* (2002) 3(10):966–74. doi:10.1038/ni837
46. Davis JM, Ramakrishnan L. The role of the granuloma in expansion and dissemination of early tuberculous infection. *Cell* (2009) 136(1):37–49. doi:10.1016/j.cell.2008.11.014
47. Egen JG, Rothfuchs AG, Feng CG, Horwitz MA, Sher A, Germain RN. Intravital imaging reveals limited antigen presentation and T cell effector function in mycobacterial granulomas. *Immunity* (2011) 34(5):807–19. doi:10.1016/j.immuni.2011.03.022
48. Flugge AJ, Timmis J, Andrews PS, Moore JW, Kaye PM. Modelling and simulation of granuloma formation in visceral leishmaniasis. *Evolutionary Computation, 2009 CEC '09; IEEE Congress.* (2009). p. 3052–9. doi:10.1109/CEC.2009.4983329
49. Beattie L, Sawtell A, Mann J, Frame TC, Teal B, de Labastida Rivera F, et al. Bone marrow-derived and resident liver macrophages display unique transcriptomic signatures but similar biological functions. *J Hepatol* (2016) 65(4):758–68. doi:10.1016/j.jhep.2016.05.037
50. Amprey JL, Im JS, Turco SJ, Murray HW, Illarionov PA, Besra GS, et al. A subset of liver NK T cells is activated during *Leishmania donovani* infection by CD1d-bound lipophosphoglycan. *J Exp Med* (2004) 200(7):895–904. doi:10.1084/jem.20040704
51. Robert-Gangneux F, Drogoul AS, Rostan O, Piquet-Pellorce C, Cayon J, Lisbonne M, et al. Invariant NKT cells drive hepatic cytokine microenvironment favoring efficient granuloma formation and early control of *Leishmania donovani* infection. *PLoS One* (2012) 7(3):e33413. doi:10.1371/journal.pone.0033413
52. Gasteiger G, Fan X, Dikiy S, Lee SY, Rudensky AY. Tissue residency of innate lymphoid cells in lymphoid and nonlymphoid organs. *Science* (2015) 350(6263):981–5. doi:10.1126/science.aac9593
53. Robinette ML, Fuchs A, Cortez VS, Lee JS, Wang Y, Durum SK, et al. Transcriptional programs define molecular characteristics of innate lymphoid cell classes and subsets. *Nat Immunol* (2015) 16(3):306–17. doi:10.1038/ni.3094
54. Juno JA, Keynan Y, Fowke KR. Invariant NKT cells: regulation and function during viral infection. *PLoS Pathog* (2012) 8(8):e1002838. doi:10.1371/journal.ppat.1002838
55. Mattarollo SR, West AC, Steegh K, Duret H, Paget C, Martin B, et al. NKT cell adjuvant-based tumor vaccine for treatment of myc oncogene-driven mouse B-cell lymphoma. *Blood* (2012) 120(15):3019–29. doi:10.1182/blood-2012-04-426643
56. Mussai F, De Santo C, Cerundolo V. Interaction between invariant NKT cells and myeloid-derived suppressor cells in cancer patients: evidence and therapeutic opportunities. *J Immunother* (2012) 35(6):449–59. doi:10.1097/CJI.0b013e31825be926
57. Pilonis KA, Aryankalayil J, Demaria S. Invariant NKT cells as novel targets for immunotherapy in solid tumors. *Clin Dev Immunol* (2012) 2012:720803. doi:10.1155/2012/720803
58. Gonzalez-Aseguinolaza G, de Oliveira C, Tomaska M, Hong S, Bruna-Romero O, Nakayama T, et al. Alpha-galactosylceramide-activated Valpha 14 natural killer T cells mediate protection against murine malaria. *Proc Natl Acad Sci U S A* (2000) 97(15):8461–6. doi:10.1073/pnas.97.15.8461
59. Chackerian A, Alt J, Perera V, Behar SM. Activation of NKT cells protects mice from tuberculosis. *Infect Immun* (2002) 70(11):6302–9. doi:10.1128/IAI.70.11.6302-6309.2002
60. Albergante L, Timmis J, Beattie L, Kaye PM. A Petri net model of granulomatous inflammation: implications for IL-10 mediated control of *Leishmania donovani* infection. *PLoS Comput Biol* (2013) 9(11):e1003334. doi:10.1371/journal.pcbi.1003334

**Conflict of Interest Statement:** JT is Director of SimOmics Ltd.; PA is employed by SimOmics Ltd.; all other authors declare no conflict of interest.

Copyright © 2018 Moyo, Beattie, Andrews, Moore, Timmis, Sawtell, Hoehme, Sampson and Kaye. This is an open-access article distributed under the terms of the Creative Commons Attribution License (CC BY). The use, distribution or reproduction in other forums is permitted, provided the original author(s) and the copyright owner are credited and that the original publication in this journal is cited, in accordance with accepted academic practice. No use, distribution or reproduction is permitted which does not comply with these terms.